Electronic Supplementary Material (ESI) for Journal of Materials Chemistry A.

Electronic Supplementary Information

Soranyel Gonzalez-Carrero, Guillermo Mínguez Espallargas, Raquel E. Galian* and Julia Pérez-Prieto*

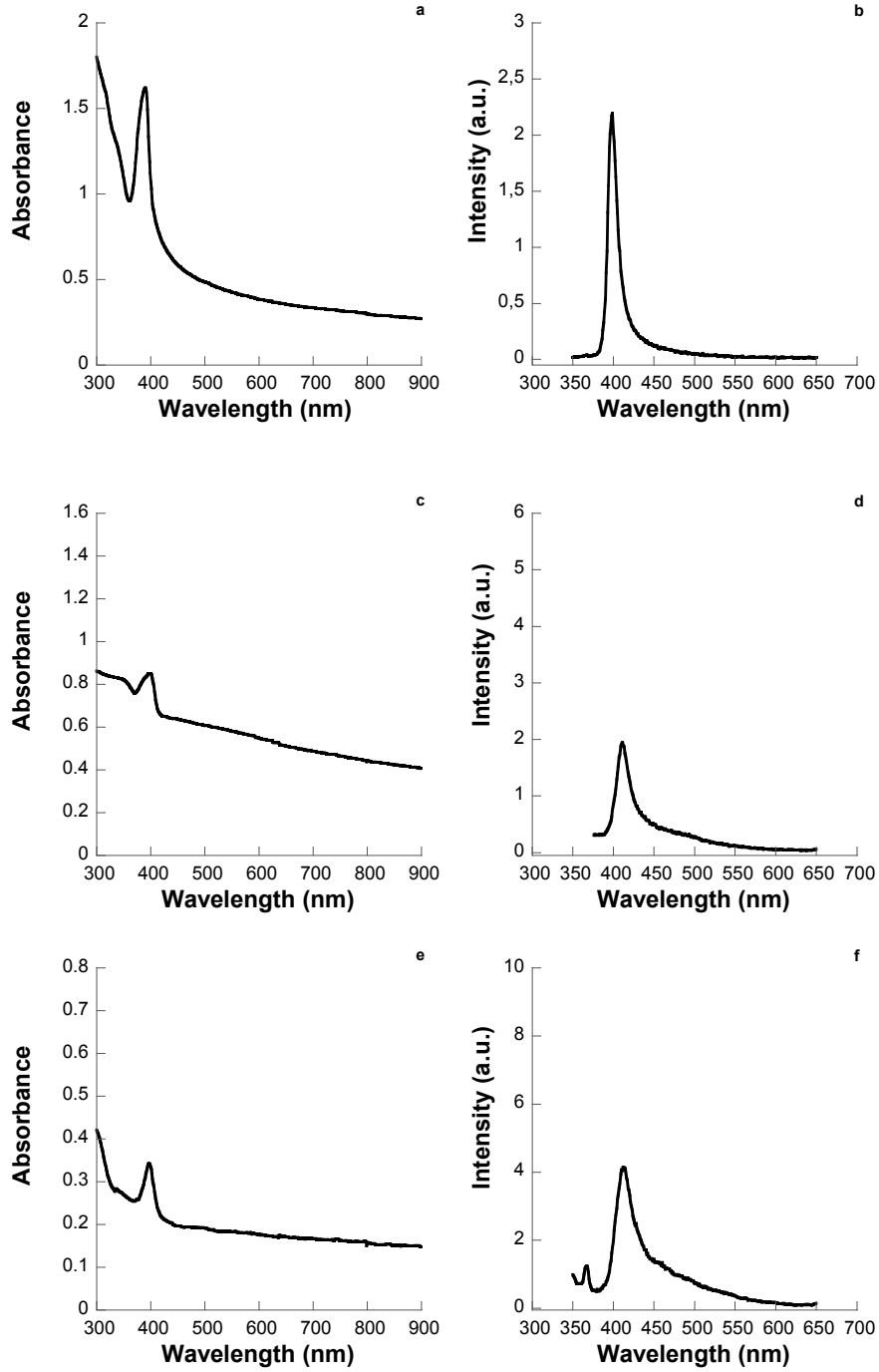

Figure S1. Absorption and emission (λ_{exc}= 330 nm) spectra of colloidal solutions of $\mathbf{P_{ODA1}}$ (1 mg/mL; a,b) $\mathbf{P_{OCA1}}$ (0.6 mg/mL; c,d), and $\mathbf{P_{HXA1}}$ (0.2 mg/mL; e,f) and in toluene.

Table S1. Emission lifetimes (τ) and their corresponding contributions (A) to the total signal of the perovskites dispersed in toluene or as a spin-coated film.

	χ	PL[a] nm	$\langle\tau_{av}\rangle$[b] ns	τ_1 ns	τ_2 ns	A_1	A_2
P_{ODA1}/air	1.19	397	9.345	3.154	30.155	96.975	3.025
P_{ODA1}/N_2	1.28	397	8.840	3.120	31.560	97.580	2.420
Film[c]	0.88	398	1.810	0.768	1.929	21.23	78.76
P_{ODA2}/air	1.40	397	4.192	2.773	27.89	99.41	0.592
P_{ODA2}/N_2	1.50	397	3.833	2.650	27.33	99.51	0.486
Film[c]	1.29	398	2.18	1.289	2.386	29.70	70.29
P_{HXA2}/air	1.01	408	6.404	2.618	24.48	97.81	2.191
P_{HXA2}/N_2	1.21	408	6.413	2.413	22.15	97.31	2.695
P_{OCA2}/air	0.95	409	3.675	2.615	22.365	99.340	0.659
P_{OCA2}/N_2	1.01	409	5.794	2.670	27.805	98.550	1.454

[a] Wavelength of the maximum emission (excitation at 340 nm); [b] τ_{av} average lifetime; [c] Film prepared by spin-coating of toluene dispersion of the perovskite on quartz.

Quantification of dispersable A_2PbBr_4 perovskites

TGA and ^{1}H-NMR analysis of the $\mathbf{P_{HXA1}}$, $\mathbf{P_{OCA1}}$, $\mathbf{P_{ODA1}}$, $\mathbf{P_{HXA2}}$, $\mathbf{P_{OCA2}}$, and $\mathbf{P_{ODA2}}$ perovskites after purification and their supernatants (**Ss**) give valuable information on the composition of these perovskites.

The first loss of weight in the perovskite samples **was** attributed to the loss of the organic capping of the material, i.e., ODE and ammonium salt (plus OLA in some samples) . The second step of the weight loss was ascribed to the loss of the ammonium bromide in the perovskite framework, while the third step is consistent with the loss of the perovskite lead bromide.

In the case of the supernatants, removal of the solvent followed by addition of ethyl ether caused the precipitation of a solid (**Ss**). In addition, the ether solution was distilled, thus recovering ODE with the ammonium salt (plus OLA in the case of the synthesis of $\mathbf{P_{HXA1}}$, $\mathbf{P_{OCA1}}$, and $\mathbf{P_{ODA1}}$). For comparative purposes, the TGA of the individual precursors (namely HXABr, OCABr, and ODABr ammmoniun salts) and the corresponding amines, as well as that of ODE, OLA, and lead bromide, were also recorded and are included in TGA section.

Further data on the composition of $\mathbf{P_{HXA}}$, $\mathbf{P_{OCA}}$ and $\mathbf{P_{ODA}}$ samples were obtained from their ^{1}H-NMR spectra, which gave information on the molar ratio of the organic components (RMN section). In combination with their TGA spectra, the $PbBr_2$ weight percentage present in the isolated mass was calculated. The ^{1}H-NMR spectra of the supernatants were also analysed (spectra not included); the data obtained from them combined with those of the corresponding perovskite samples were consistent with the amount of material used in the preparation of the perovskites.

The molar composition of $\mathbf{P_{ODA1}}$, $\mathbf{P_{ODA2}}$, $\mathbf{P_{HXA2}}$, and $\mathbf{P_{OCA2}}$, as well as the yield of isolated perovskite (estimation based on the mmol of $PbBr_2$ in the perovskite compared to the mmol used in the reaction) are shown in Tables **S2-S4**.

Thermogravimetric Analysis Section

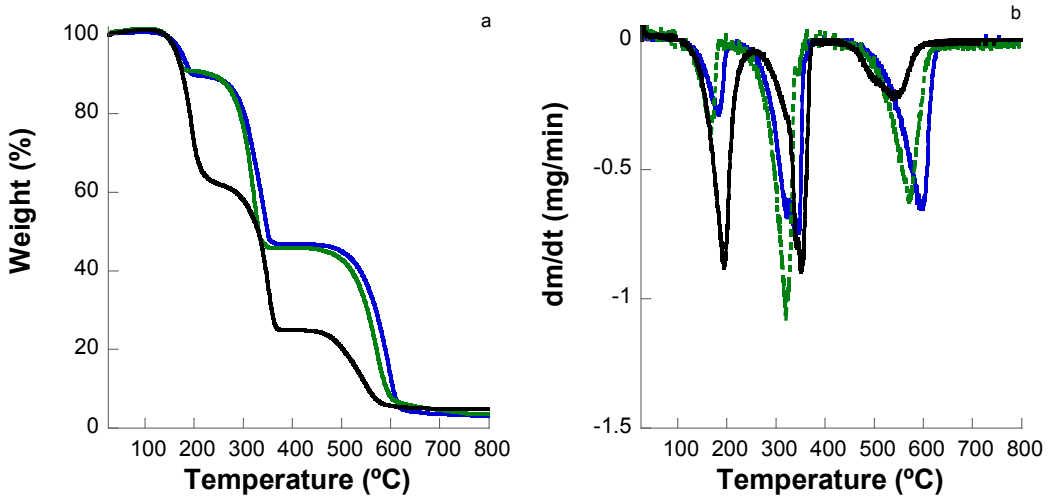

Figure S2. TGA heating curves of $\mathbf{P_{HXA1}}$ (-), $\mathbf{P_{OCA1}}$ (-) and $\mathbf{P_{ODA1}}$ (-) expressed as weight % as a function of applied temperature (a) and the corresponding 1st derivate (b).

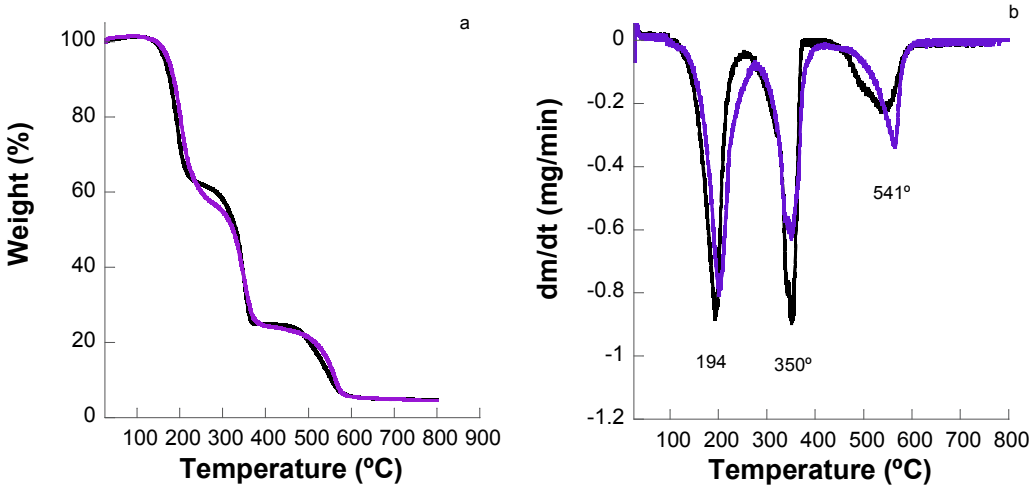

Figure S3. Comparison of TGA heating curves of $\mathbf{P_{ODA1}}$ (-) and $\mathbf{P_{ODA2}}$ (-) expressed as weight % as a function of applied temperature (a) and the correspondin1st derivate (b).

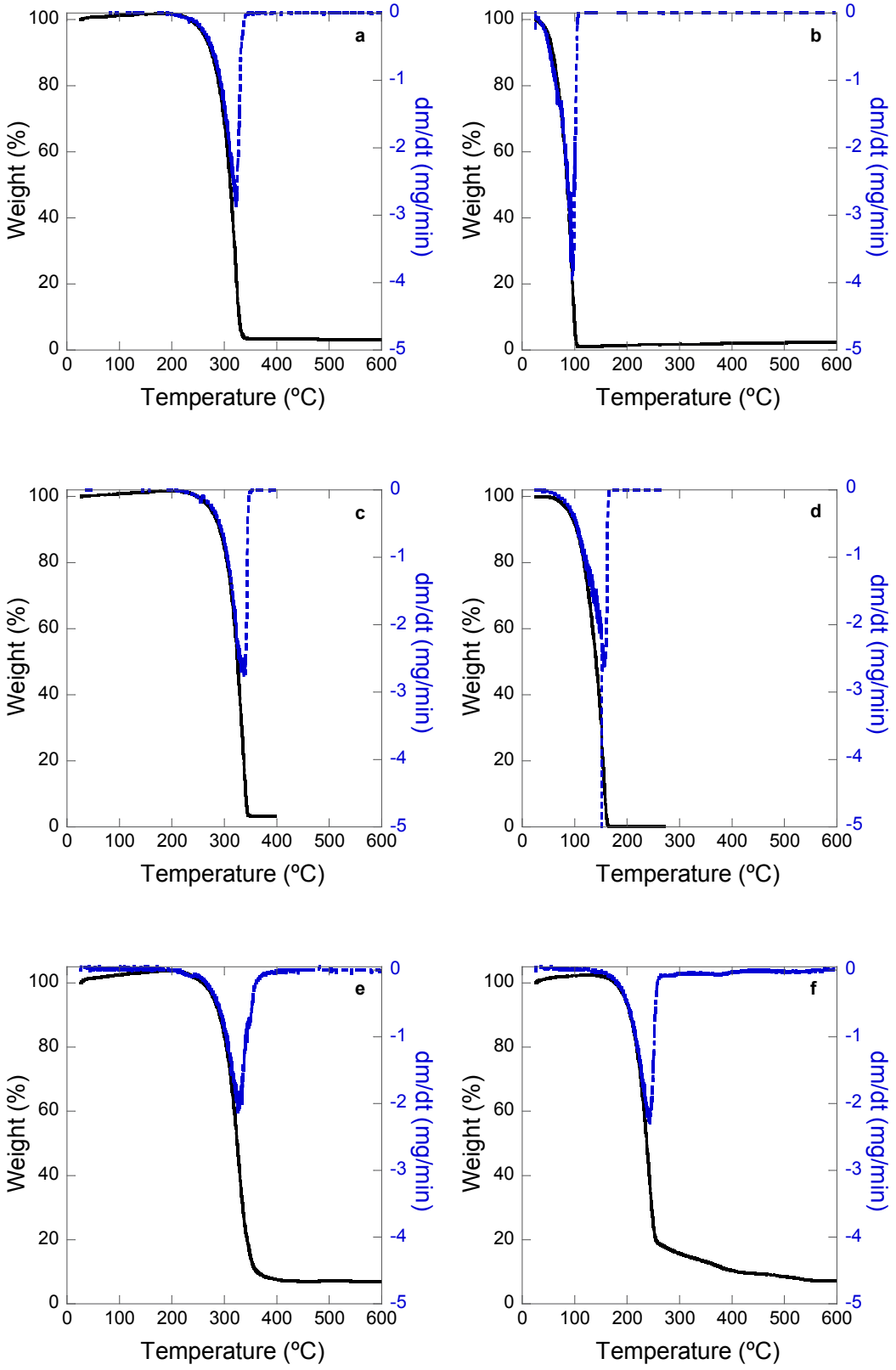

Figure S4. TGA heating curves of **HXABr** (a), hexyl amine **HXA** (b), **OCABr** (c) octylamine **OCA** (d), **ODABr** (e) and octadecylamine **ODA** (f) expressed as weight % as a function of applied temperature and the corresponding1st derivate.

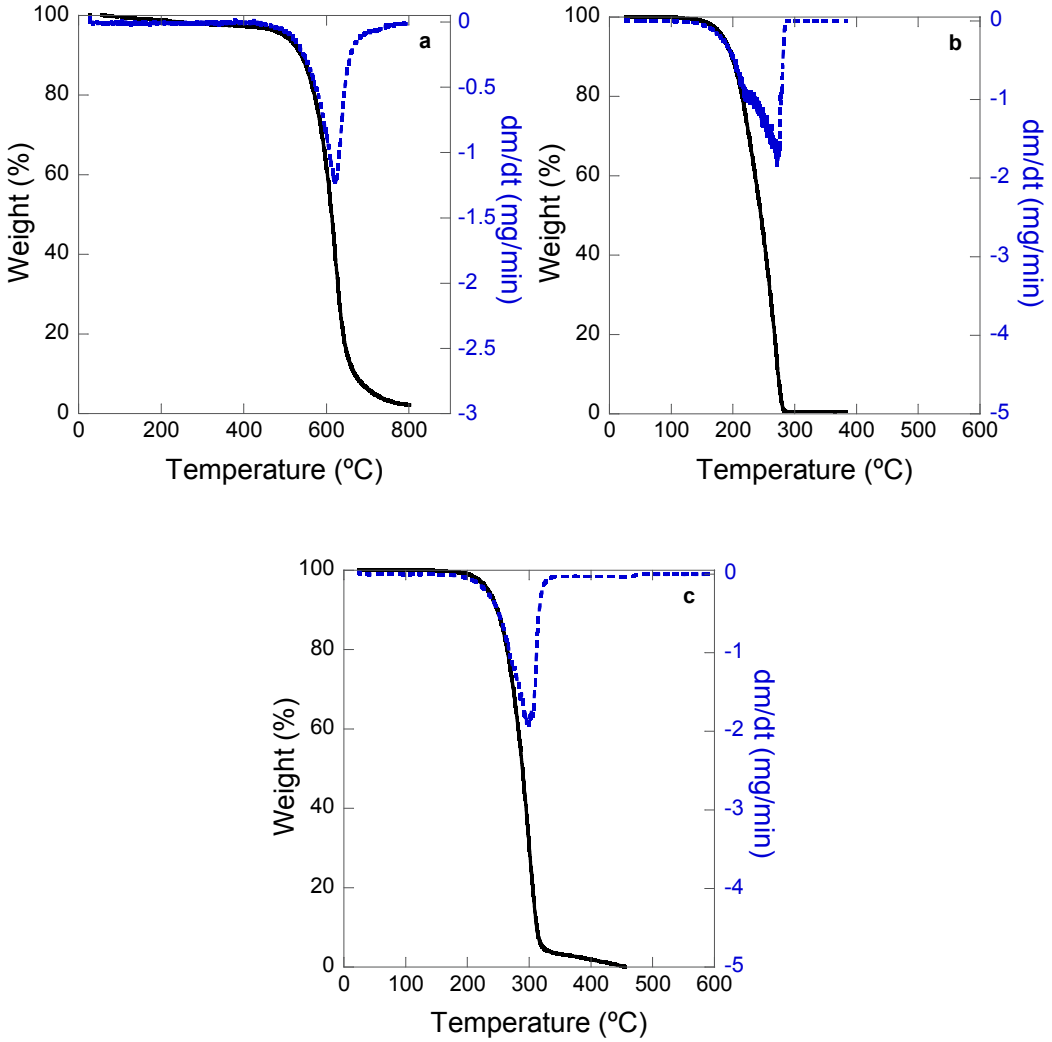

Figure S5. TGA heating curve of lead bromide (a) **ODE** (b) and **OLA** (c) expressed as weight % as a function of applied temperature and the corresponding1st derivate.

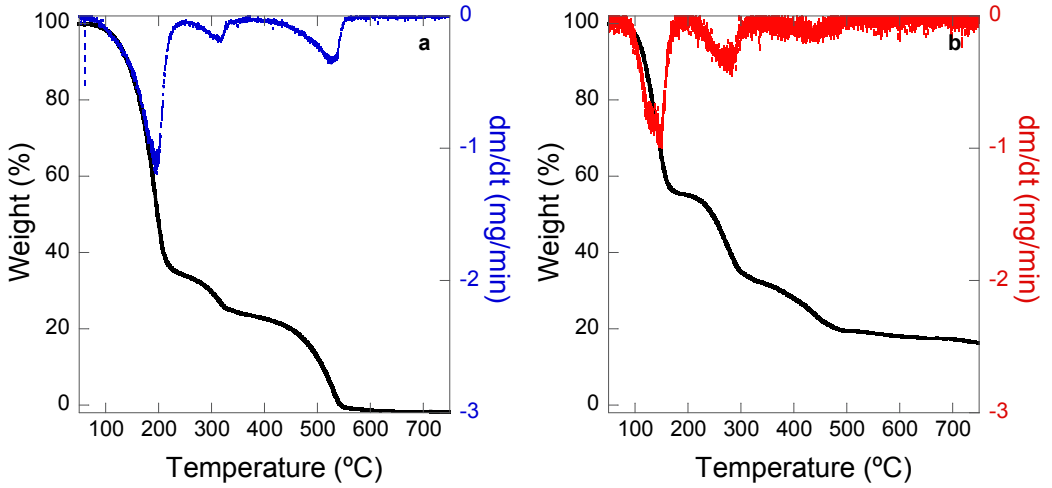

Figure S6. TGA heating curves expressed as weight % as a function of applied temperature and the corresponding1st derivate of $\mathbf{P_{ODA1}}$ **Ss** (a) and $\mathbf{P_{ODA2}}$ **Ss** (b)

[1]H -RMN section

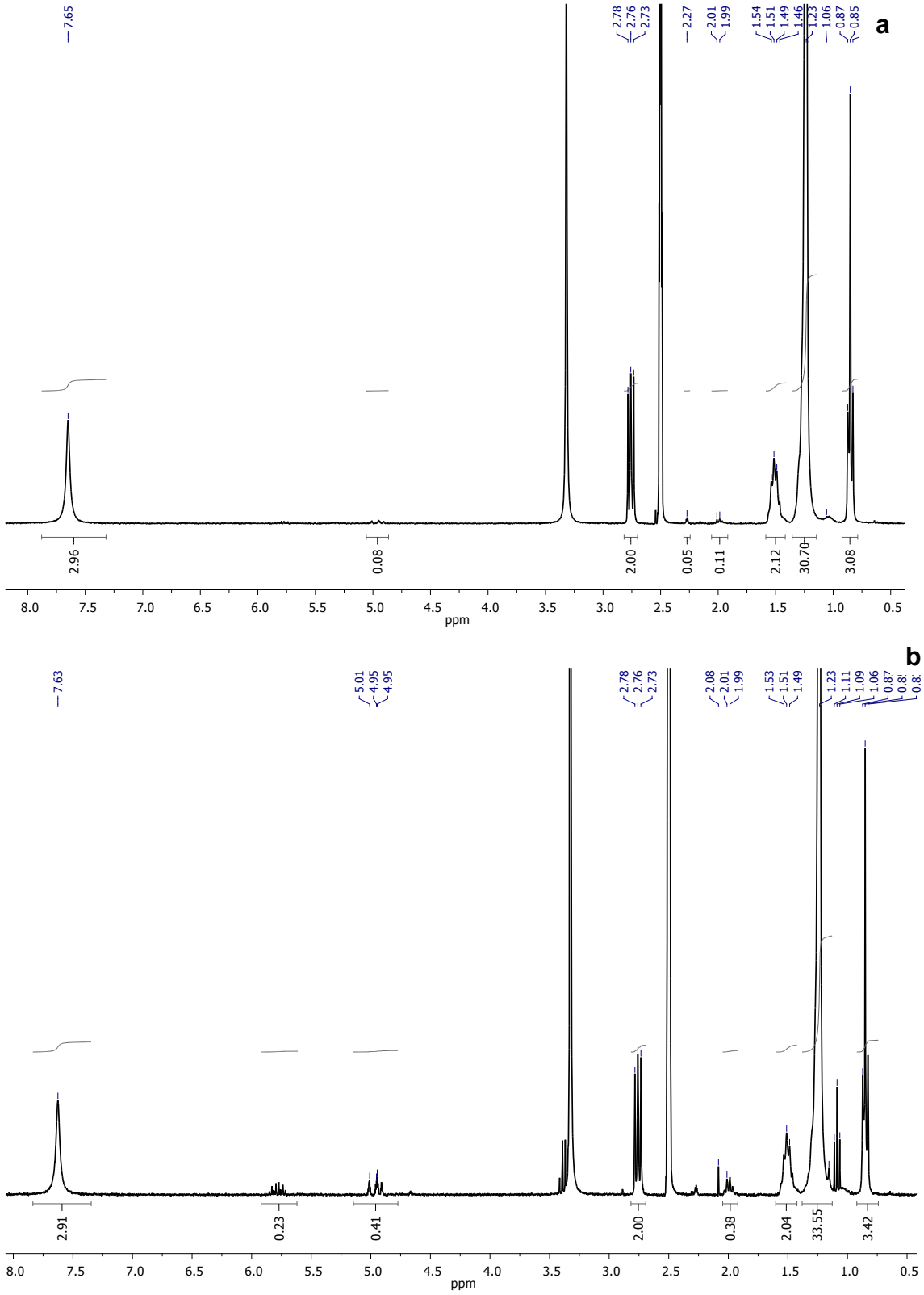

Figure S7. [1]H-RMN (300 MHz) spectrum of $\mathbf{P_{ODA1}}$ (a) and $\mathbf{P_{ODA2}}$ (b) in deuterated DMSO.

Octylammonium bromide

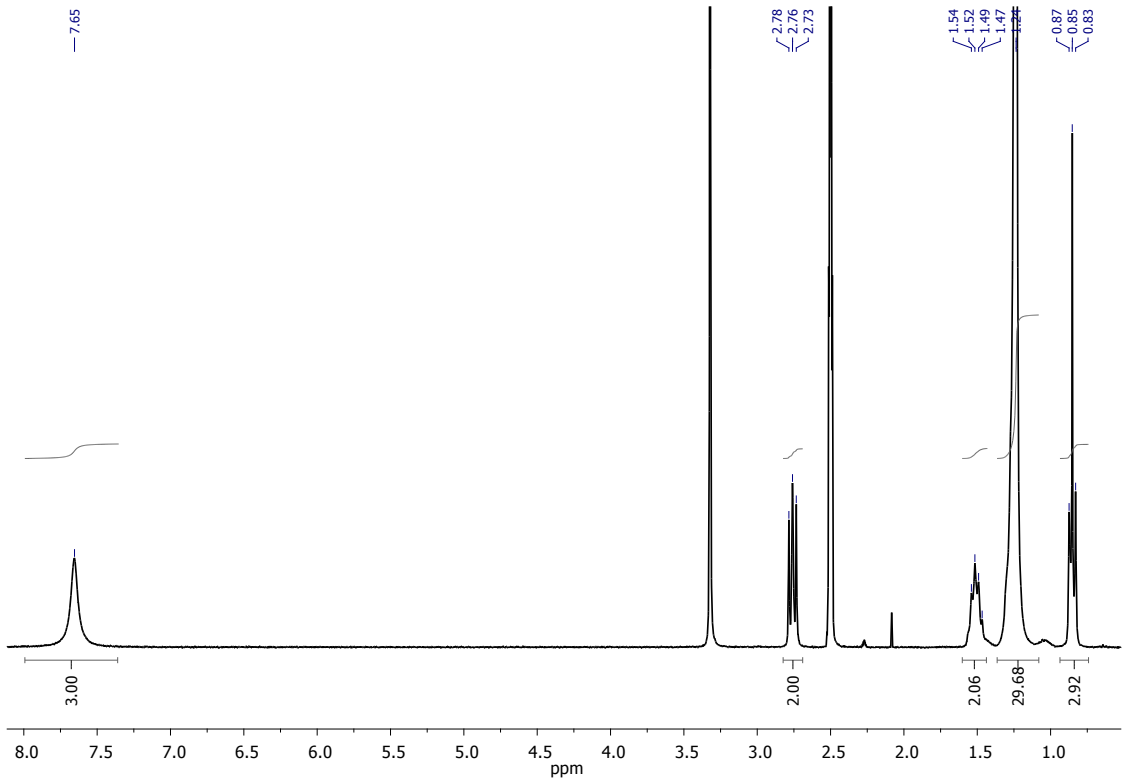

Figure S8. ^{1}H NMR (300 MHz) spectrum of octylammonium bromide (**ODABr**) in deuterated DMSO.

^{1}H NMR (300 MHz, d-DMSO) (300 MHz, DMSO) δ 7.65 (s, 3H), 2.76 (t, J = 7.7 Hz, 2H), 1.60 – 1.44 (m, 2H), 1.24 (s, 30H), 0.85 (t, J = 6.7 Hz, 3H).

Oleic acid

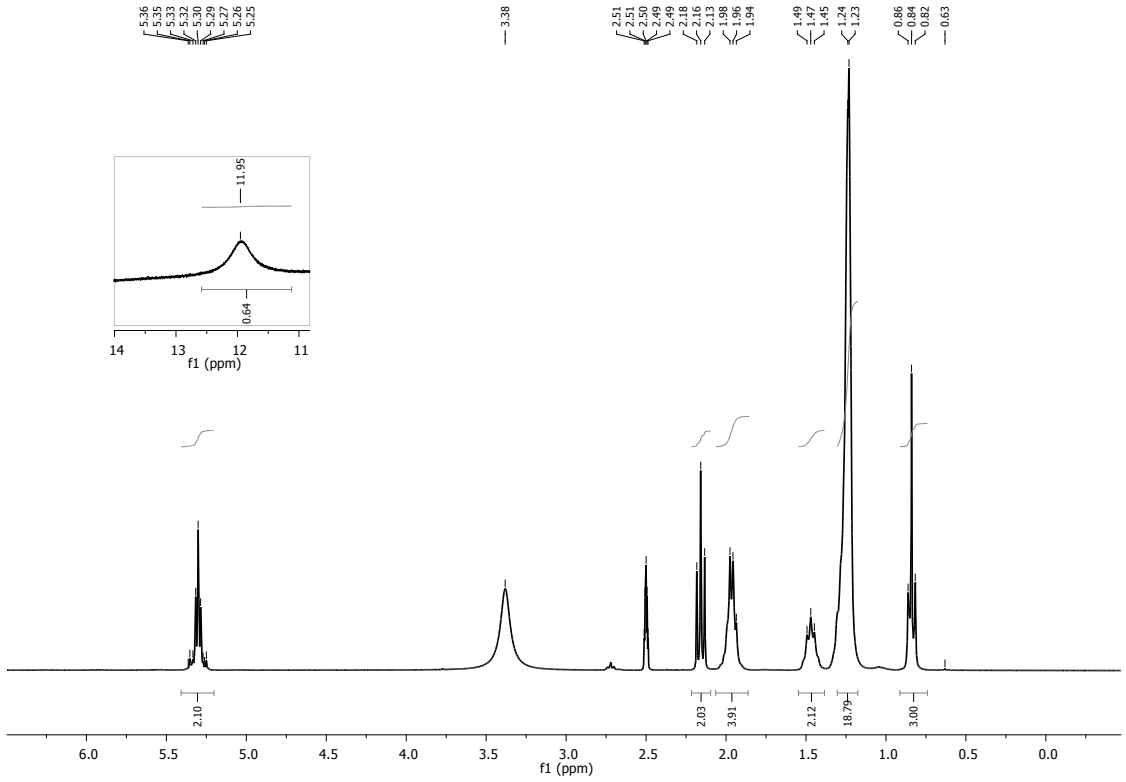

Figure S9. ^{1}H NMR (300 MHz) spectrum of oleic acid (**OLA**) in deuterated DMSO.

^{1}H NMR (300 MHz, d-DMSO) δ 11.95 (s, 1H), 5.41 – 5.20 (m, 2H), 2.16 (t, J = 7.4 Hz, 2H), 2.06 – 1.86 (m, 4H), 1.55 – 1.38 (m, 2H), 1.23 (d, J = 2.3 Hz, 19H), 0.91 – 0.74 (m, 3H).

Octadecene

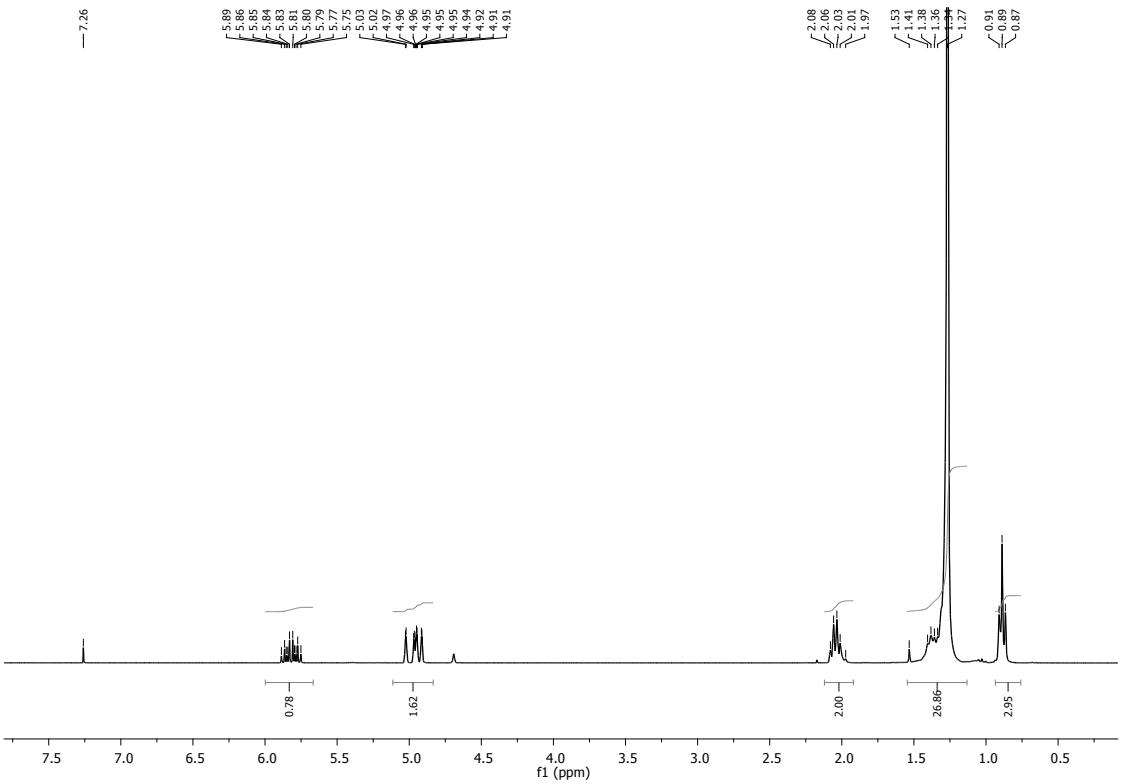

Figure S10. ^{1}H NMR (300 MHz) spectrum of **ODE** in deuterated $CDCl_3$.

^{1}H NMR (300 MHz, $CDCl_3$) δ 5.82 (ddt, J = 16.9, 10.2, 6.7 Hz, 1H), 5.12 – 4.76 (m, 2H), 2.12 – 1.92 (m, 2H), 1.60 – 0.97 (m, 27H), 0.89 (t, J = 6.6 Hz, 3H).

Table S2. Quantification of the component molar ratio in $\mathbf{P_{ODA1}}$

Reagents	Reagents [a] mmol	P_{ODA1}	
		Component [b] mmol	Component/$PbBr_2$ [b] Molar ratio
ODABr surfactant	0.20	0.081	**175**
ODABr framework		0.077	**1.86**
ODE	6.09	0.004	**0.09**
OLA	0.26		
$PbBr_2$	0.10	0.044	**1.00**

[a] Moles used in the synthesis. [b] Moles of each component in the product calculated by TGA and ^{1}H-RMN; perovskite chemical yield of 44%.

Table S3. Quantification of the component molar ratio in $\mathbf{P_{ODA2}}$

Reagents	Reagents[a] mmol	P_{ODA2}	
		Component [b] mmol	Component/$PbBr_2$ [b] Molar ratio
ODABr surfactant	0.10	0.053	**1.77**
ODABr framework		0.053	**1.77**
ODE	3.00	0.011	**0.36**
$PbBr_2$	0.05	0.030	**1.00**

[a] Moles used in the synthesis. [b] Moles of each component in the product calculated by TGA and ^{1}H-RMN; perovskite chemical yield of 60%

Table S4. Quantification of the component molar ratio in $\mathbf{P_{OCA2}}$

Reagents	Reagents[a] mmol	P_{OCA2}	
		Component [b] mmol	Component/$PbBr_2$ [b] Molar ratio
OCABr surfactant	0.20	0.029	**0.40**
OCABr framework		0.135	**1.82**
ODE	6.10	0.003	**0.04**
$PbBr_2$	0.10	0.074	**1.00**

[a] Moles used in the synthesis. [b] Moles of each component in the product calculated by TGA and ^{1}H-RMN; perovskite chemical yield of 74% .

X-Ray Photoelectron Spectroscopy Section

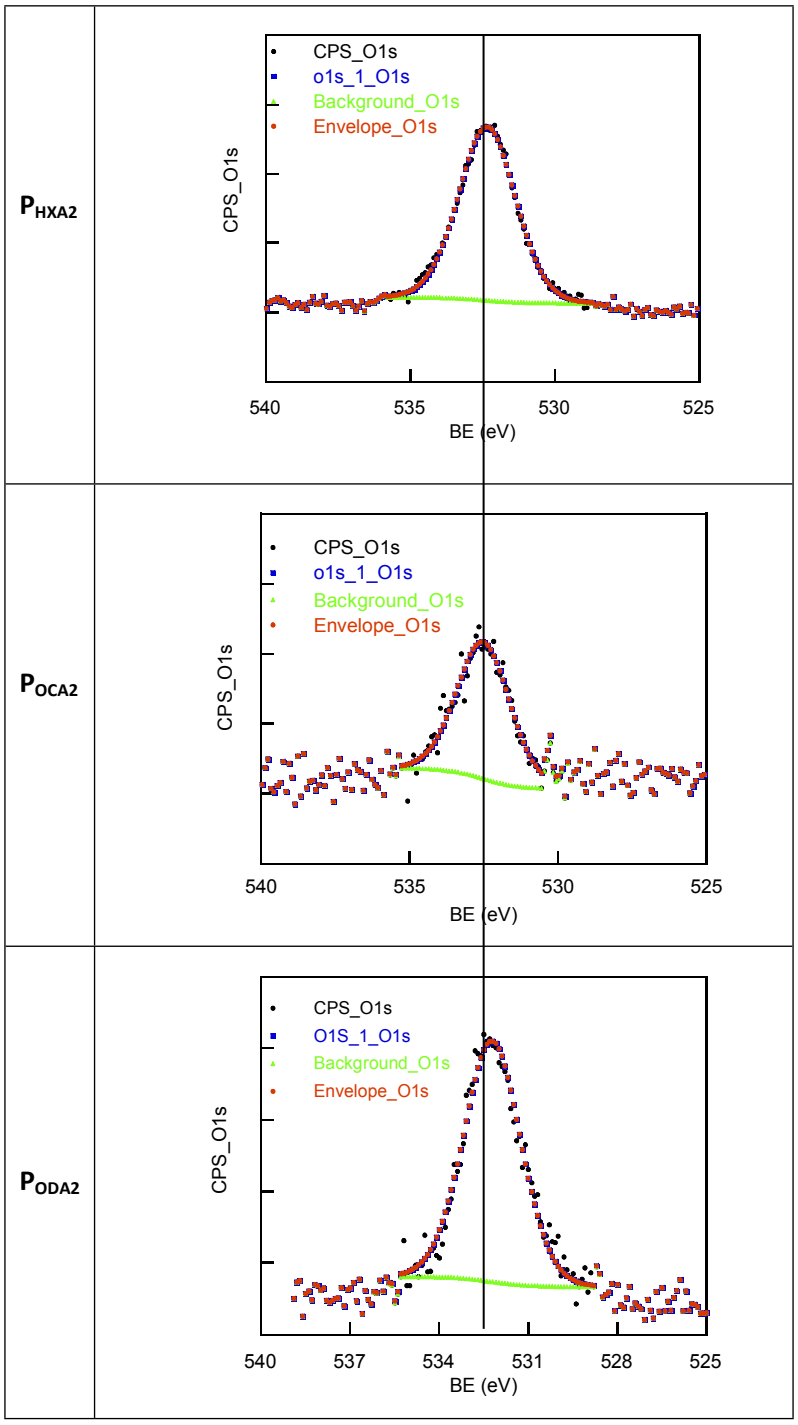

Figure S11. XPS spectra of O_{1s} for $\mathbf{P_{HX2}}$, $\mathbf{P_{OCA2}}$ and $\mathbf{P_{ODA2}}$

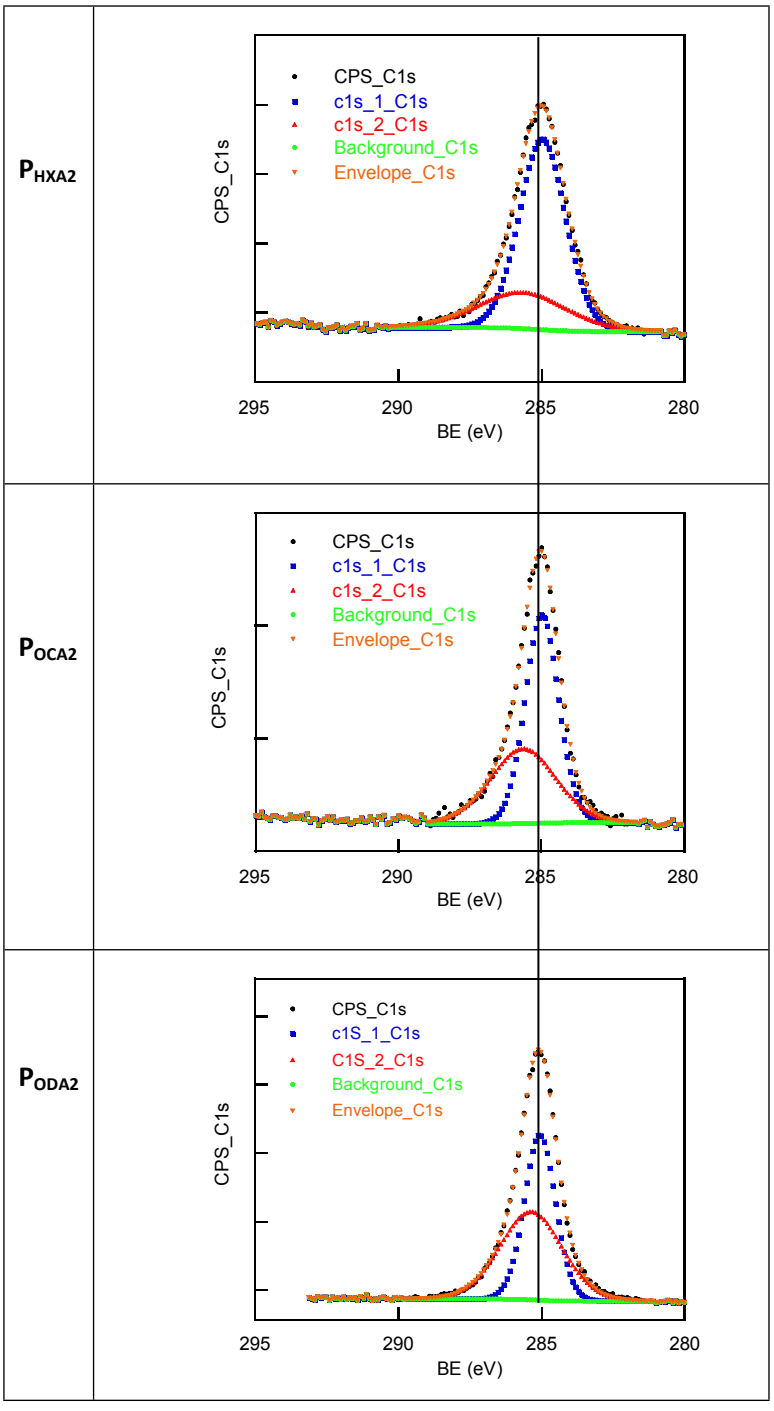

Figure S12. XPS spectra of C_{1s} for $\mathbf{P_{HXA2}}$, $\mathbf{P_{OCA2}}$ and $\mathbf{P_{ODA2}}$

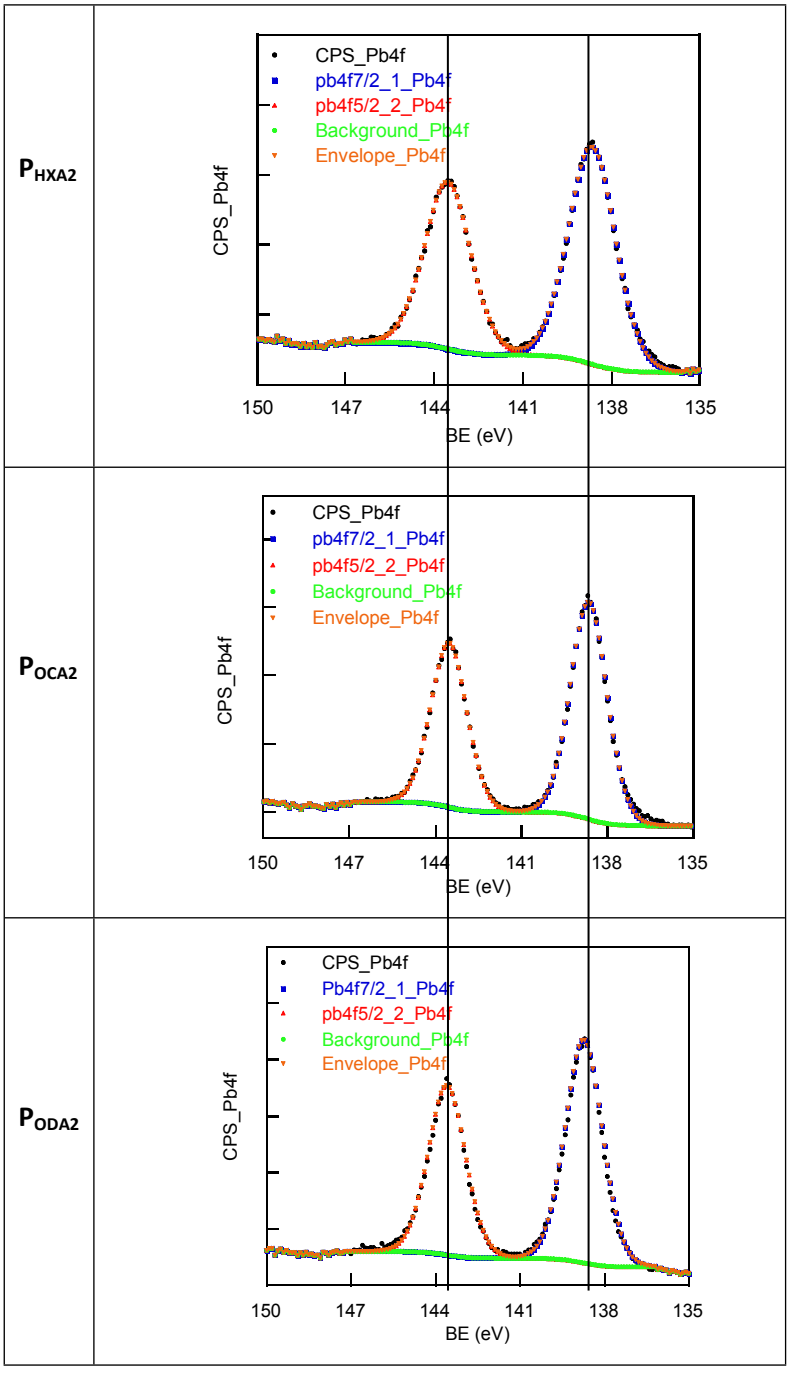

Figure S13. XPS spectra of Pb_{4f} for $\mathbf{P_{HXA2}}$, $\mathbf{P_{OCA2}}$ and $\mathbf{P_{ODA2}}$

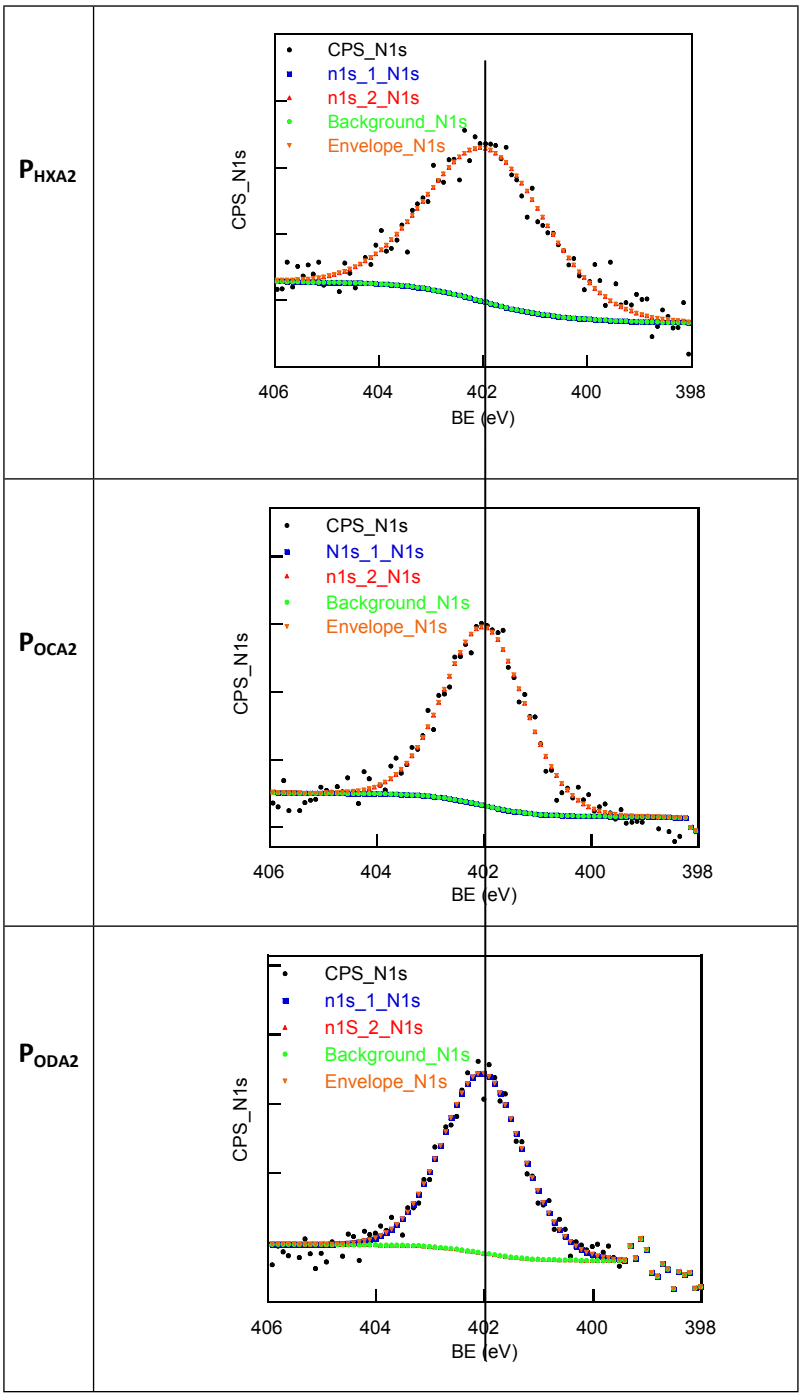

Figure S14. XPS spectra of N_{1s} for $\mathbf{P_{HXA2}}$, $\mathbf{P_{OCA2}}$ and $\mathbf{P_{ODA2}}$

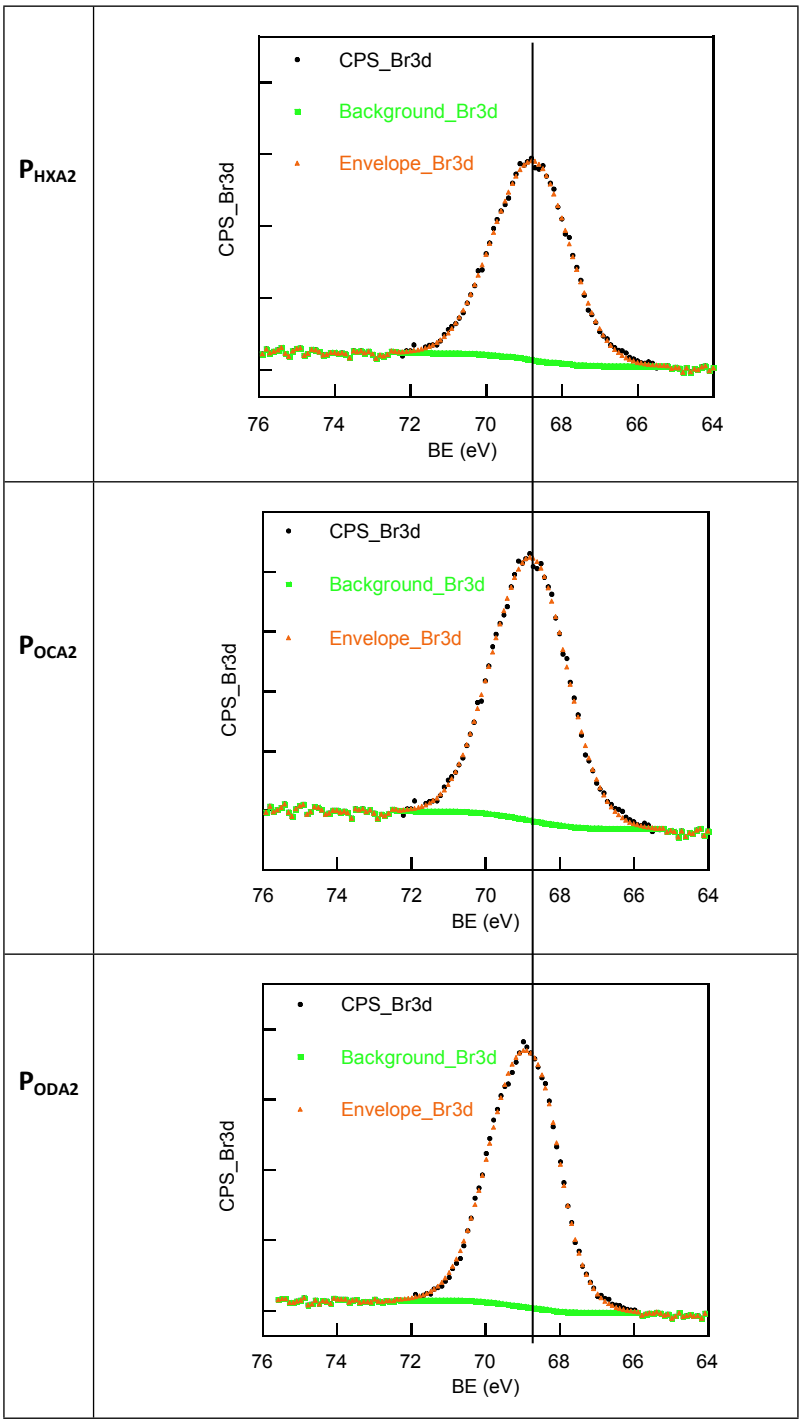

Figure S15. XPS spectra of Br_{3d} for $\mathbf{P_{HXA2}}$, $\mathbf{P_{OCA2}}$ and $\mathbf{P_{ODA2}}$

Transmission electron microscopy Section

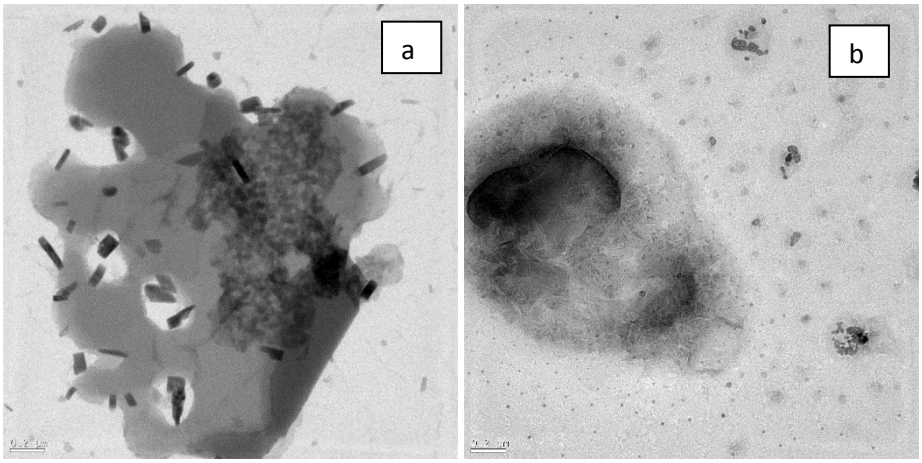

Figure S16. HRTEM of $\mathbf{P_{HXA2}}$ (a) and $\mathbf{P_{OCA2}}$ (b). Scale bar 0.2 μm.

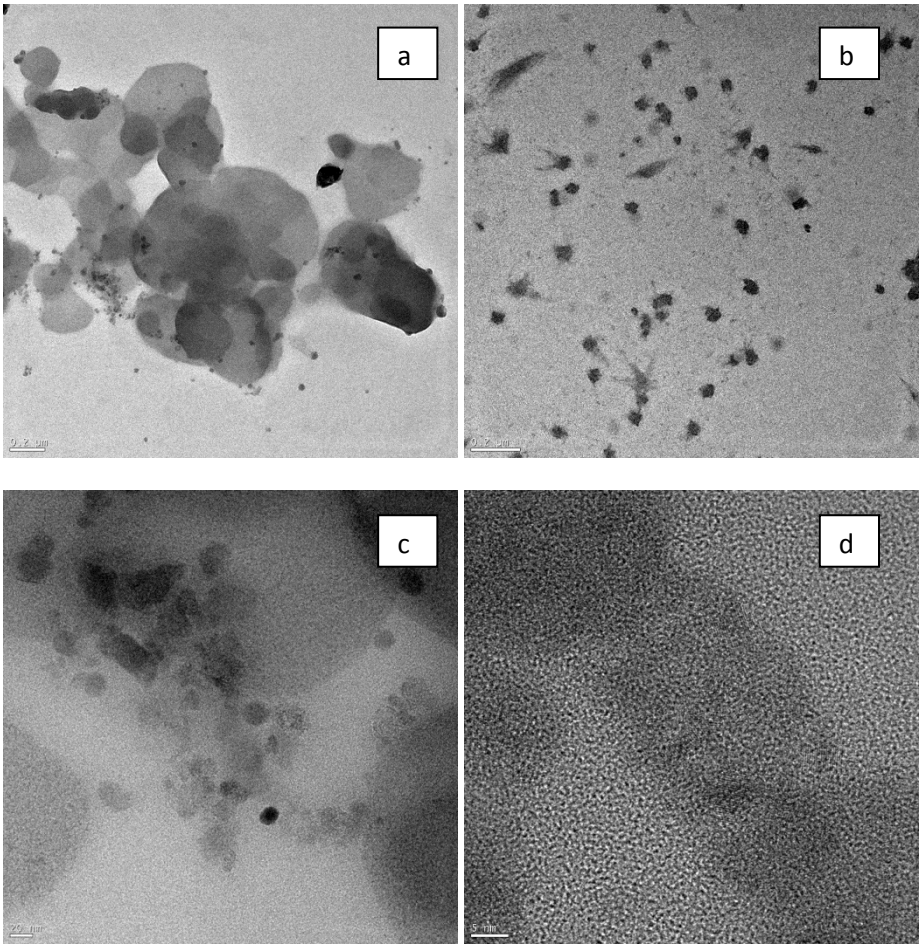

Figure S17. HRTEM of $\mathbf{P_{ODA2}}$ in toluene. Scale bar 0.2 μm (a,b), 20 nm (c) and 5 nm (d)**.**

X-ray Diffraction Section

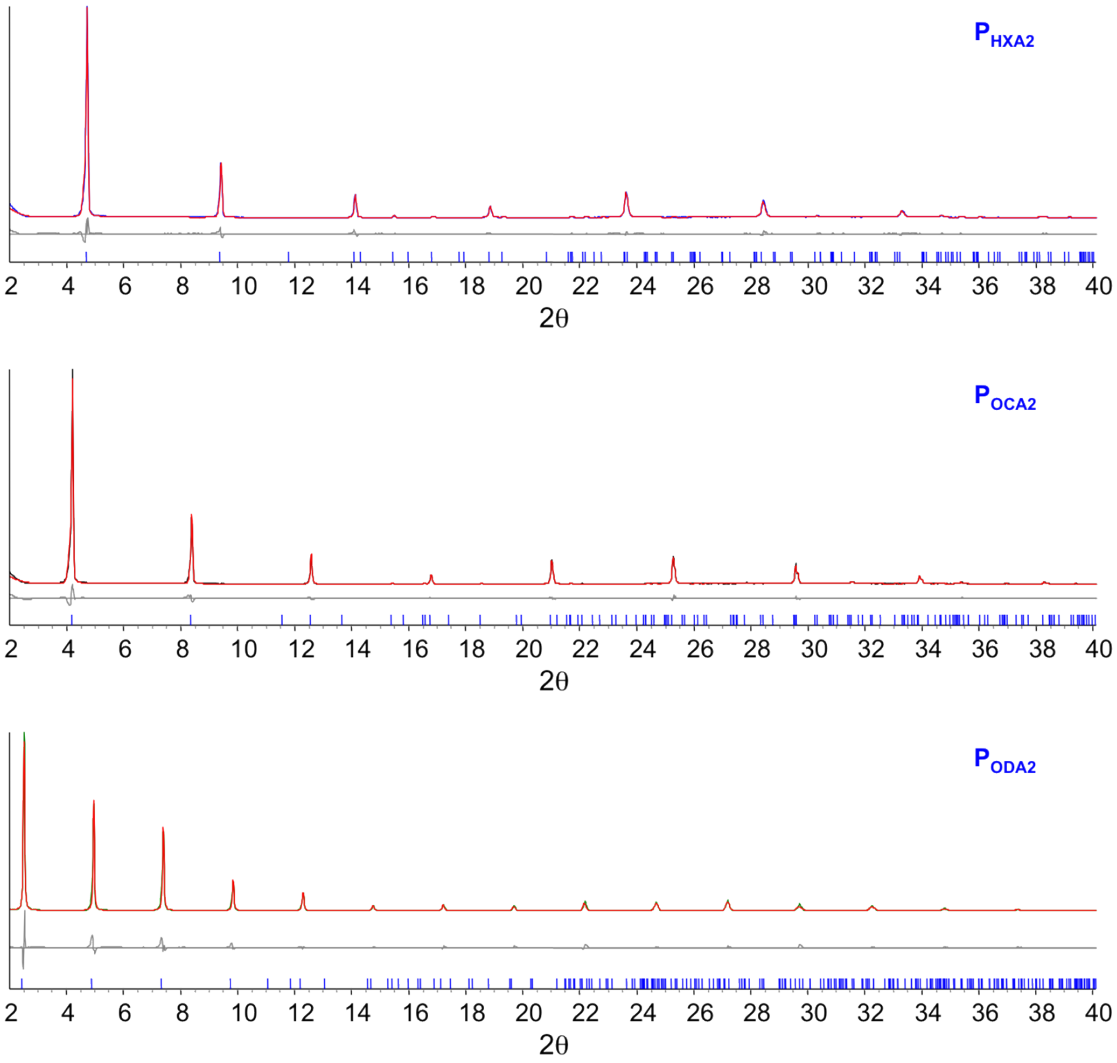

Figure S18. Observed (*blue*) and calculated (*red*) profiles and difference plot [(I_{obs} – I_{calcd})] (*grey*) of the X-ray powder diffraction Pawley refinement for **P_{HXA2}** (top), **P_{OCA2}** (middle) and **P_{ODA2}** (bottom) (λ = Cu Kα, 2θ range 2.0–40.0 °); tick marks indicate peak positions.

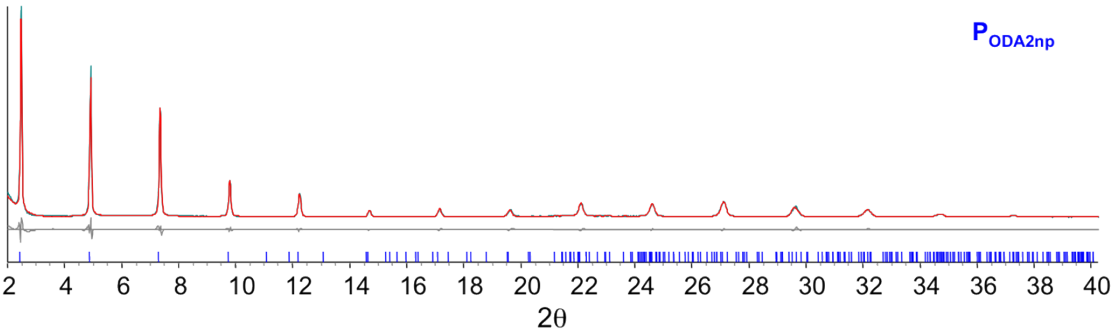

Figure S19. Observed (*blue*) and calculated (*red*) profiles and difference plot [(I_{obs} – I_{calcd})] (*grey*) of the X-ray powder diffraction Pawley refinement after processing, **P_{ODA2np}** (λ = Cu Kα, 2θ range 2.0–40.0 °); tick marks indicate peak positions.

Photostability Studies

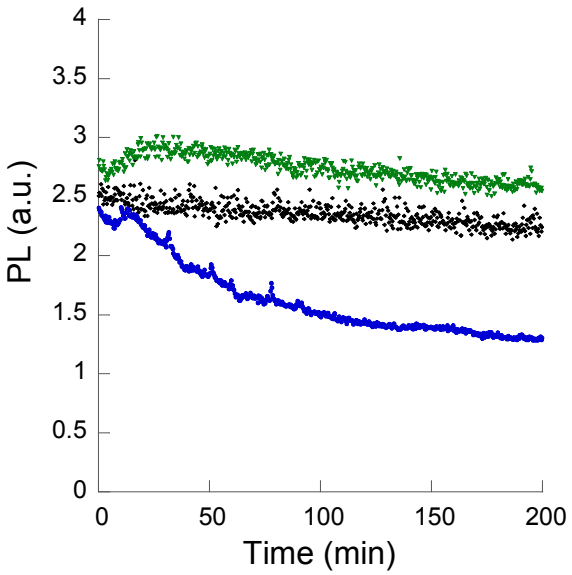

Figure S20. Photoluminescence of $\mathbf{P_{HXA2}}$ (■), $\mathbf{P_{OCA2}}$ (▼) and $\mathbf{P_{ODA2}}$ (♦) dispersed in toluene as a function of the irradiation time (λ_{exc}= 330 nm), PL registered at 411, 409, and 397 nm, respectively, under nitrogen atmosphere.